JOURNAL OF MATERIALS SCIENCE 32 (1997) 4061–4070

Kinetic equations for diffusion-controlled precipitation reactions

M. J. STARINK
Centre de Thermodynamique et de Microcalorimétrie du CNRS, 13331 Marseille Cedex 3, France

In the past it has been suggested that the Johnson-Mehl-Avrami Kolmogorov (JMAK) equation can be used to describe the progress of a large number of nucleation and growth reactions, including diffusion-controlled precipitation reactions, provided that nucleation is random. However, its validity has only been proved for reactions with a linear growth and not for diffusion-controlled precipitation reactions. Here, the ability of the JMAK equation to fit the experimental data of diffusion-controlled precipitation reactions has been compared with the Austin–Rickett (AR) equation

$$\alpha = 1 - \{[k(T)t]^n + 1\}^{-1}$$

In all cases studied the AR equation provides a better fit to the data and the obtained integer and half-integer values of n can be interpreted in terms of the physics of the transformation processes. The latter is mostly not possible for n values obtained from the JMAK equation. It is concluded that for the purpose of interpreting data of precipitation reactions, the AR equation is more appropriate than the JMAK equation.

1. Introduction

In the study of the transformations which proceed via nucleation and growth, several mathematical descriptions of the amount transformed as a function of the time, or the transformation rate as a function of the amount transformed, have been suggested in the literature. The best known description finds its roots in the late 1930s when its basis was laid independently by several researchers (Johnson and Mehl [1], Avrami [2–4] and Kolmogorov [5]). It has since been referred to as the Johnson–Mehl–Avrami–Kolmogorov (JMAK), the Johnson–Mehl–Avrami (JMA) or simply the Avrami kinetic equation. Although these early researchers originally derived the theory only for specific cases (in his original derivation, Avrami only considered spherical transformed regions growing proportional to time in all three dimensions), later the JMAK theory was generalized to include a large number of reaction types, and it has been suggested that it is also valid for diffusion-controlled precipitation reactions (see, for instance, [6]). In the generalized form, the JMAK equation gives the fraction transformed, α, as a function of the time, t

$$\alpha = 1 - \exp\{-[k(T)t]^n\} \quad (1)$$

where n is a constant often referred to as the Avrami exponent, and $k(T)$ is a temperature-dependent factor. Recently, it was proved [7] that for reactions progressing via random nucleation (i.e. the probability of the formation of a nucleus is constant everywhere in the untransformed volume) and linear growth, the JMAK equation is exact over the entire range of α. For this type of reaction, $n = 4$. Nevertheless, in cases where comparisons of recrystallization experiments with the JMAK equation were published, often the correspondence was found to be limited to small α values (see [8, 9]). A possible explanation for this discrepancy may be found in a nucleation rate which varies with the position in the sample [10].

For diffusion-controlled growth, Ham [11, 12] stated that, even though it provides a good approximation for low fractions transformed, the JMAK equation has no fundamental importance. Recently, Lee and Kim [13] obtained several kinetic equations by introducing, in addition to the parameters $k(T)$ and n, an adjustable fitting parameter termed the "impingement factor", c. They showed that $c = 0$ corresponds to JMAK kinetics, whilst for $c = 1$ the following equation was obtained

$$\alpha = 1 - \{[k(T)t]^n + 1\}^{-1} \quad (2)$$

The above equation has been first proposed by Austin and Rickett [14]. Lee and Kim showed that the Austin–Rickett (AR) equation fitted the transformation data for the formation (precipitation) of bainite plates in two shape-memory alloys very well. This finding suggests that the AR equation is more appropriate than the JMAK equation for the study of precipitation reactions.

To study the validity of the AR equation and to compare it with the JMAK theory, the ability of the JMAK and the AR equation to fit experimentally

Present address: IPTME, University of Technology, Lougborough LE11 3TU, UK.

0022–2461

obtained transformation curves of a large number of precipitation reactions, have been compared. The values of n obtained for the various reactions have been discussed and the status of the JMAK and the AR equation assessed. The derivation of these equations is reviewed.

2. Derivation of kinetic equations

2.1. The fraction transformed in the JMAK "extended volume" concept

Similar to the works of Johnson and Mehl [1] and Avrami [2–4], the transformation is described using the so-called "extended volume" concept. In the "extended volume", the individual nuclei grow without any limitation of the space, i.e. growth is not inhibited by impingement. In applying this concept first the volume, V_p, of a single particle at time, t, which nucleated at an earlier time, z, is obtained

$$V_p = A_1[G(t-z)]^m \quad (3)$$

where G is the growth rate, A_1 and m are constants related to the dimensionality of the growth and the mode of transformation. Values of A_1 and m have been given in various works on nucleation and growth [6]. For example, for a polymorphic reaction with the product phase growing as spheres, $m = 3$ and $A_1 = 4\pi/3$. Also for diffusion-controlled growth, Equation 3 is valid (see [6]). For instance, for particles which grow in three dimensions by diffusion of the atoms through the surrounding matrix, $m = 1\frac{1}{2}$. More examples are given in Tables I and II.

Next the contribution of nucleation is considered. In the derivation of the original JMAK theory, it has been assumed that the amount of nuclei formed in volume V_0 during a time interval dz is given by $I(z)V_0 dz$, where $I(z)$ is the nucleation rate per unit volume at time z. Several authors have pointed out that this apparently leads to the creation of nuclei in the already transformed part of the material. These nuclei have been termed "phantom nuclei". Erukhimovitch and Baram [15, 16] argue that it is necessary to compensate for this effect by adding a term $(1-\alpha)$ to the nucleation rate. A fundamental problem with the addition of the $(1-\alpha)$ term is that the creation of phantom nuclei really should be considered as an impingement problem, and should not be corrected for in this stage where transformation in the extended volume is considered. Thus phantom nuclei will be considered in Section 2.2 as a part of an impingement problem. (In addition, computer calculations performed by the present author indicate that the addition of the $(1-\alpha)$ term to correct for phantom nuclei has a very limited effect on the overall transformation rate and can in no way explain the difference between Equations 1 and 2.)

Now the contribution of the particles which nucleated during the time interval $(z,\ z+dz)$ to the amount of transformed volume in the "extended volume" at time t, $V_{ext}(t)$ is obtained by using Equation 3

$$dV_{ext} = A_1 I(z) V_0 [G(t-z)]^m dz \quad (4)$$

TABLE I Values of n for several diffusion-controlled reactions (see, for instance, [6, 11, 12, 41])

Conditions and geometries	Nucleation rate	
	Zero ($n=m$)	Constant
All particles growing from small dimensions	$1\frac{1}{2}$	$2\frac{1}{2}$
Growth of long cylinders with constant length	1	2
Growth of large plates with constant surface area	$\frac{1}{2}$	$1\frac{1}{2}$
Growth of grain-boundary (GB) particles, high diffusivity in GB	$\frac{1}{2}$	$\frac{1}{2}$
Growth of particles, initial size large compared to changes due to growth	$\frac{1}{2}$	–
Growth on dislocations	$\frac{2}{3}$	–

TABLE II Values of n for polymorphic changes, recrystallization, discontinuous precipitation, eutectoid reactions, interface controlled growth, etc (see, for instance, [6, 41])

Conditions and geometries	Nucleation rate	
	Zero ($n=m$)	Constant
All particles growing in three dimensions starting from small size	3	4
All particles growing in two dimensions starting from small size	2	3
All particles growing in one dimension starting from small size	1	2
Grain-boundary nucleation after saturation		1

Integrating and introducing $\alpha_{ext} = V_{ext}/V_0$ yields

$$\alpha_{ext} = \int_0^t A_1 I(z)[G(t-z)]^m dz \quad (5)$$

For several expressions of the nucleation rate, $I(z)$, analytical expressions for Equation 5 can be obtained. If the nucleation rate is constant during the entire transformation, one obtains

$$\alpha_{ext}\ (I = \text{constant}) = A_2 I G^m t^{m+1} \quad (6)$$

where A_2 is a constant. When all nuclei are formed whilst α is still negligible, i.e. when the nucleation rate is zero during practically the entire transformation, α_{ext} is given by

$$\alpha_{ext}\ (I = 0) = A_3 G^m t^m \quad (7)$$

where A_3 is a constant. Hence, this case arises for the limit of $I(z)$ decreasing infinitely fast, and it can, for instance, arise when the number of nucleation sites is limited and all sites are used for nucleation very early on in the transformation. This case has been referred to as "site saturation", and this term is adopted in this work. Hence, for both cases (Equations 6 and 7) one obtains

$$\alpha_{ext} = [k(T)t]^n \quad (8)$$

with $k(T)$ a temperature-dependent factor determined by A_2, G and I, or (for the site saturation case) A_3 and G. Also for $I(z) \sim t^a$ with a an integer larger than unity,

Equation 5 results in an expression like Equation 8 (with in this case $n = m + 1 + a$). However, it seems that for an isothermal experiment a continuously increasing nucleation rate is unrealistic, and that an increasing nucleation rate can realistically only occur as a transient effect in the very first stages of the reaction. (However, if nucleation occurs at well-defined heterogeneous nucleation sites, such as, for instance, dislocations, whilst the number of these sites increases with time, an increasing nucleation rate could be possible.) Of more practical importance is the case of a decreasing nucleation rate. As Equations 6 and 7 are the limiting cases for a constant I and an infinitely fast decreasing I, it is possible that the case of a decreasing nucleation rate corresponds to Equation 8 with $m < n < m + 1$. However, this can only be the case for specific functions $I(z)$; for example, if I decreases from I_0 at $\alpha = 0.01$ to I_e at $\alpha = 0.99$ there is only one function $I(z)$ that results in α_{ext} being given by a function of the type in Equation 8. Hence, for a decreasing nucleation rate, in specific cases Equation 8 might still hold, but in general no such simple relation is valid. Various authors have considered which values n can take (see [6]). Some of these results are presented in Tables I and II.

2.2. Impingement

Next the problem of impingement is considered. Several authors (see [3, 6, 15, 16]) have shown that in order to derive the JMAK equation, one must assume that the actual transformed volume, V_t, and the extended volume are related through

$$dV_t = \left(1 - \frac{V_t}{V_0}\right) dV_{ext} \quad (9)$$

which is equivalent to

$$\frac{d\alpha}{d\alpha_{ext}} = (1 - \alpha) \quad (10)$$

and which results in

$$1 - \alpha = \exp(-\alpha_{ext}) \quad (11)$$

From the latter equation and Equation 8, the JMAK equation (Equation 1) is readily derived.

As mentioned before, it can be proved [7] that the above approach is correct when nucleation is random and growth is linear, but no such proof exists for diffusion-controlled growth. In fact, the following two examples show that for diffusion-controlled reactions, the JMAK approach to impingement is invalid. Consider, first, a diffusion-controlled reaction for which nucleation in the undepleted part of the alloy is random. As nucleation will be dependent on solute concentration, it is clear that, in this case, random nucleation throughout the volume cannot be maintained beyond the point where a significant part of the matrix becomes significantly depleted of solute. In this stage of the reaction, nucleation will be strongly place-dependent, which violates an assumption in the JMAK treatment. For a second example, a zero nucleation rate (i.e. site saturation) is considered. Ham [11, 12] has shown that for a regular array of precipitates growing by diffusion through the surrounding matrix, Equation 10 underestimates the impingement effect. For a less-regular distribution, it is expected that impingement of diffusion fields will occur earlier on in the transformation and that hence for an irregular distribution precipitate impingement will be even stronger than for the regular array. So independently of whether the precipitates are situated on a regular array or distributed in a less-regular matrix, Equation 10 underestimates the impingement effect.

In an alternative approach of the impingement problem, Lee and Kim [13] considered impingement to be described by

$$\frac{d\alpha}{d\alpha_{ext}} = (1 - \alpha)^{1+c} \quad (12)$$

where c is an "impingement parameter". For $c = 0$ one obtains the JMAK equation, whilst for $c = 1$ (i.e. a stronger impingement effect as compared to the JMAK treatment) the AR equation (Equation 2) is obtained. The latter provided a good fit for the precipitation of bainite plates in two shape-memory alloys over a wide temperature range (180–300 °C). In view of this finding and of the reasoning in the previous paragraph, it is thought that the AR equation is more appropriate than the JMAK equation for diffusion-controlled reaction.

In Fig. 1 the results of the impingement treatment according to the JMAK model (i.e. Equation 10) and the impingement treatment according to Equation 12 with $c = 1$ (resulting in the AR equation) are compared. This figure shows that up to α about 0.2, the two treatments give results that are practically indistinguishable. For higher values of α, the difference between the two treatments increases markedly.

2.3. Grain-boundary nucleation and growth of pre-existing particles

Generally, a single transformation may occur via different nucleation processes. For instance, nucleation may occur preferentially at grain corners or grain boundaries, before nucleation in the grain interior

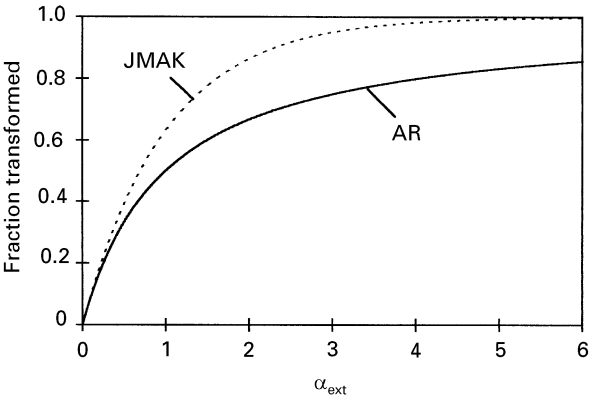

Figure 1 Fraction transformed, α, versus α_{ext} describing impingement according to the two models (the JMAK model and the AR equation).

becomes important. To account for these effects, the following relatively simple expansion of the theory presented above is proposed.

When two types of precipitation processes occur, α_{ext} is given by

$$\alpha_{ext} = \int_0^t C_1 I_1(z)[G(t-z)]^{m_1} dz + \int_0^t C_1 I_2(z)[G(t-z)]^{m_2} dz \quad (13)$$

where the symbols have the same meanings as before, whilst subscripts 1 and 2 stand for processes 1 and 2. For the case where both processes occur, via either constant nucleation rate or site saturation, it follows that

$$\alpha_{ext} = k_1(T)t^{n_1} + k_2(T)t^{n_2} \quad (14)$$

The relation between α and α_{ext} is again assumed to be given by Equation 12.

3. Comparison of kinetic equations with experiments

Equations 1 and 2 are now compared with data on several precipitation reactions which proceed by nucleation and diffusion-controlled growth. The examples were selected mainly from past publications by the present author, work in progress and work performed in groups in which the author worked and is familiar with. Three main criteria were used for selection: (i) transformation data should be available over the entire range of α, (ii) scatter should be low, (iii) curves should be sigmoidal on a logarithmic time scale. It is stressed that once selected for study on the basis of these criteria, none was later omitted from this publication. Hence, although somewhat biased towards the field of expertise of the author (most of the transformations studied are transformations in aluminium-based alloys), the selected examples are in no way biased towards any of the two theories presented. The theory predicts that n values should be integer or half integer. Hence, unless noted, only integer or half integer values of n are used in the fitting of the experimental data.

3.1. Formation of the equilibrium δ (AlLi) phase in Al–Li

Noble and Thompson [17] have studied the precipitation during isothermal ageing of the equilibrium δ (AlLi) phase in Al–Li alloys using resistivity measurements. The fraction transformed during ageing of an Al–2 mass % Li alloy at 300 °C is presented in Fig. 2. Neither the JMAK equation nor Equation 2 were able satisfactorily to fit the entire transformation.

As the overall evolution of the fraction transformed in the Al–2 mass % Li alloy is thought to be due to a combination of grain-boundary precipitation and precipitation in the grain interior (see next Section), Equations 12 and 14 were used to fit the data. Using $n_1 = \frac{1}{2}$ and $n_2 = 2\frac{1}{2}$, a very good fit can be obtained

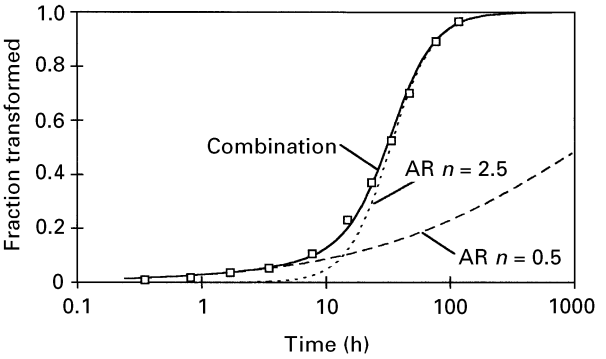

Figure 2 Fraction transformed during the formation of the δ (AlLi) phase in Al–2 mass % Li at 300 °C fitted by a model which takes both nucleation on grain boundaries and nucleation in grains into account (the combination of Equations 12 and 14).

using these equations (see Fig. 2). Two other curves in Fig. 2 are based on the assumption that solely one of the two processes occurs, and that hence Equation 2 is valid. The same procedure with α_{ext} determined by two processes according to Equation 14 but with the relation between α and α_{ext} according to the JMAK method (i.e. Equation 11), also yields a good fit with the data (results not presented), provided $n_2 = 1\frac{1}{2}$.

3.2. Precipitation in an Al–Si alloy

Van Mourik and co-workers [18, 19] studied the precipitation in melt-spun Al–Si alloys by means of lattice parameter measurements. The lattice parameter of the aluminium-rich phase in binary Al–Si is a linear function of the amount of silicon dissolved in it [20], and hence the lattice parameter is a linear function of the fraction transformed. By estimating the start and the end value of the lattice parameter from a set of data, the fraction transformed can be obtained. Using Fig. 4 in [18], this has been done for precipitation in the Al–10.3 at % Si alloy aged at 124 °C; results are presented in Fig. 3. When only integer and half-integer values of n are considered, the best fitting curve for the JMAK equation is obtained for $n = 1$ and for the AR equation with $n = 1\frac{1}{2}$. Both fits show significant deviation from the experimental values (see Fig. 3), but the overall quality of the fit, as measured by the average squared deviation between experimental points and fit, $\overline{(\Delta\alpha)^2}$, is better for the fit with the AR equation (for the JMAK fit, $\overline{(\Delta\alpha)^2} = 1.7 \times 10^{-3}$, whilst for the fit with the AR equation, $\overline{(\Delta\alpha)^2} = 1.3 \times 10^{-3}$). When n is not limited to integer and half-integer values, the difference between the quality of the fits obtained with the two equations increases markedly, and with the AR equation for $n = 1.3$, a quite good fit ($\overline{(\Delta\alpha)^2} = 0.4 \times 10^{-3}$) can be obtained.

3.3. Precipitation in an Al–Si–Cu alloy

The present author and co-workers studied the precipitation in solution-treated and quenched Al–19.1 at % Si–1.3 at % Cu alloys by means of lattice parameter

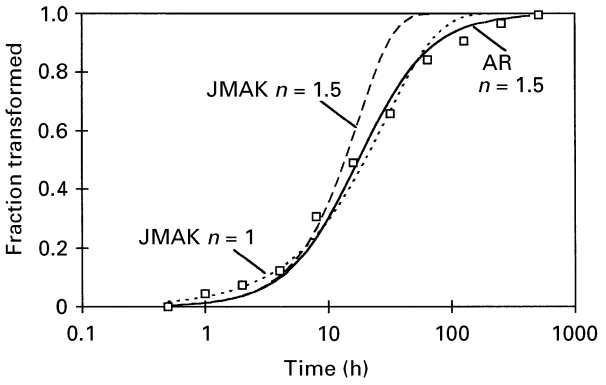

Figure 3 Fraction transformed during the ageing of a liquid-quenched Al–10.3 at % Si (11 mass %) alloy. Ageing temperature 124 °C. The quality of the fit with the AR equation, as measured by the average squared deviation between experimental points and fit, is somewhat better as compared to the fit with the JMAK equation (data from [18]).

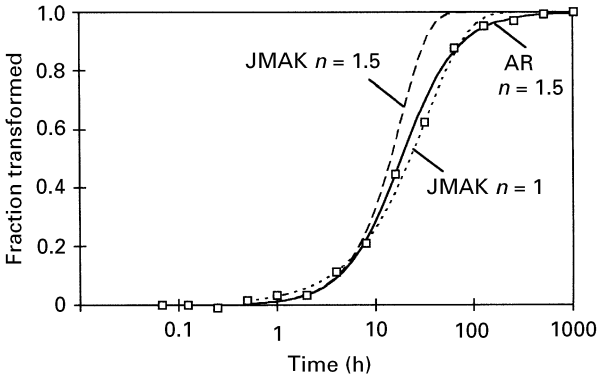

Figure 4 Fraction transformed during the ageing of a solution-treated and quenched Al–19.1 at % Si–1.3 at % Cu alloy. Ageing temperature is 150 °C (data from [21]).

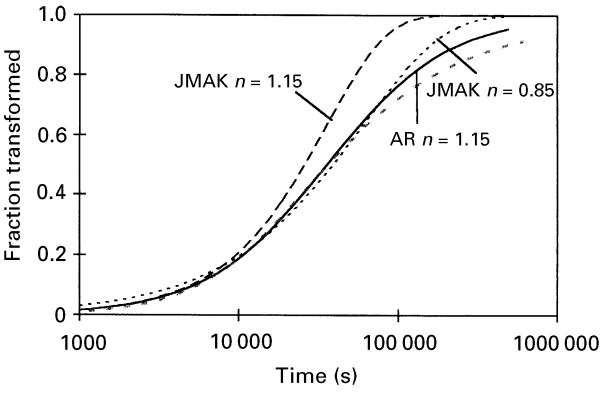

Figure 5 Fraction transformed during the formation of the Ll_2 ordered phase in Al–15Mg at 80 °C.

measurements [21]. As for Al–Si, the aluminum-rich phase lattice parameter in Al–Cu is a linear function of the amount of dissolved alloying element [22, 23], whilst experiments on an Al–1 at % Cu–1 at % Si alloy have indicated that in the ternary alloy the effects of dissolved silicon and copper on the lattice parameter are additive [21]. There are strong indications that the precipitation of copper in the form of the θ' (Al_2Cu) phase and the precipitation of silicon in the form of pure silicon (diamond structure) are linked processes [24], with the formation of silicon-phase precipitates inducing the formation of copper-rich precipitates. Hence it can be expected that the lattice parameter change is proportional to the amount of silicon precipitated. Thus, analogous to the Al–Si alloy, the fraction of silicon precipitated can be obtained from the changes of the measured lattice parameters. Fig. 4 shows that the AR equation with $n = 1\frac{1}{2}$ gives a near perfect fit to the data. The best fit for the JMAK equation is obtained for $n = 1$, but this fit is worse than that with the AR equation.

3.4. Formation of the Ll_2 ordered phase in Al–Mg and Al–Li

In Al–Mg alloys at low temperatures, an Ll_2 ordered phase can form. In the literature this precipitate has been referred to as β'' phase or as Guinier–Preston (GP) zones. The formation of this precipitate at 80 and 85 °C has been studied recently by Zahra and Starink [25] using isothermal calorimetry. For this, Al–15Mg samples were solution-treated and air-cooled to room temperature before being introduced into the calorimeter which was stabilized at the ageing temperature. A full description of the procedures for the calorimetry experiments has been presented elsewhere [26]. Selected-area diffraction on transmission electron microscopy (TEM) samples revealed that the observed exothermic heat effect is due to the formation of the Ll_2 ordered phase. From the calorimetry curves the fraction transformed was calculated (to do this an extrapolation of the heat flow to long time is necessary, see [26]; the result is presented in Fig. 5. Fitting with integer and half integer values of n gave unsatisfactory results. In Fig. 5, fitted curves for optimized n values are presented. It is clear that again the AR equation gives the better result.

Apart from the formation of the Ll_2 ordered phase in Al–15Mg discussed above, transformation data concerning the formation of Ll_2 ordered (δ') phase in Al–2 mass % Li (Fig. 12 in [17]) and the Ll_2 ordered phase in melt-spun Al–16 at %Mg (Fig. 7b in [27]) were also fitted with the JMAK equation and the AR equation. In both cases, the AR equation provided a better fit to the data.

3.5. Internal nitriding of an Fe–2 at % Al alloy

Biglari *et al.* [28] studied the mass change due to internal nitriding of a recrystallized and cold-worked, binary Al–2 at % Al alloy by holding it in a NH_3/H_2 gas mixture inside a thermobalance. Under the experimental conditions (partial pressures, temperatures) used in this work, the mass change of the sample is due to the formation of AlN precipitates in the alloy. In these experiments thin ($\leq$0.1 mm) samples were used which ensured that the concentration of dissolved nitrogen in the sample is constant, i.e. the reaction rate is not determined by nitrogen diffusion through the sample.

The fraction transformed during isothermal nitriding of the recrystallized alloy at 545 °C (818 K) is given in Fig. 6. Biglari *et al.* [28] limited their analysis to $\alpha < 0.4$ and found that for these low α values the JMAK equation with $n = 3.7$ provided a reasonably good fit. This finding is confirmed in the present work, but it is stressed that for $\alpha > 0.4$ this type of fit is very bad. The fits presented in Fig. 6 show that using the JMAK equation, the best fit for the entire range of α is obtained for $n \approx 2.5$, whilst with the AR equation the best fit is obtained for $n = 4$. Again the quality of the fit is better with the AR equation. (The fit can be improved further by taking for n the non-integer value 3.9.)

The fraction transformed during nitriding of a cold-worked Fe–2 at % Al alloy at 530 °C (803 K) is given in Fig. 7. Fitting of the JMAK equation for the entire range of α results in $n = 1$. Biglari *et al.* [28] obtained the same value by fitting the JMAK equation for $\alpha = 0.4$–0.9. However, fitting with the AR equation results in better quality fits and, for $n = 1\frac{1}{2}$, the fit is nearly perfect for $\alpha \leq 0.8$ (see Fig. 7). For $\alpha > 0.8$, deviations are observed from the latter fit. However, inspection of curves obtained by Biglari *et al.* [28] at other temperatures shows that for this range of α, the curve obtained at 530 °C has an unusually steep part (i.e. unusually high reaction rates) as compared to the other curves. Hence this deviation is not characteristic and is significantly reduced if another temperature was chosen. (However, at the other temperatures studied, curves could only be obtained for $\alpha > 0.2$ and these curves cannot be used for a fit for the entire range of α including this important low-α range.) In conclusion, for cold-worked Fe–2 at % Al the AR equation also yields the better fit, and n equals $1\frac{1}{2}$ is obtained.

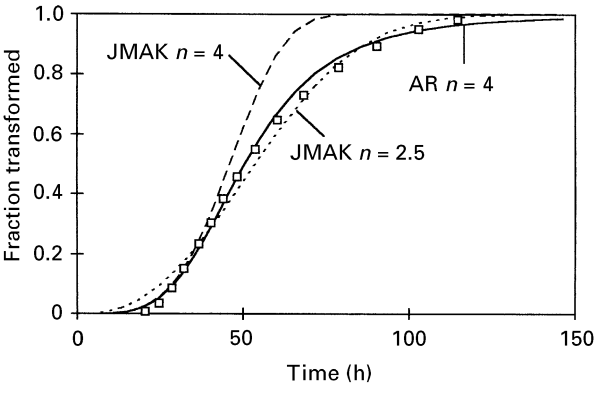

Figure 6 Fraction transformed during internal nitriding of a recrystallized Fe–2 at % Al alloy (data from [28]).

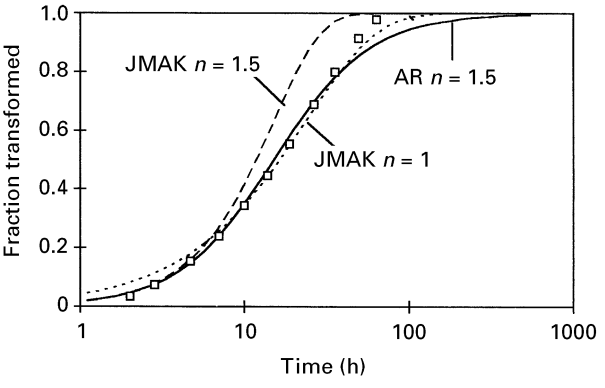

Figure 7 Fraction transformed during internal nitriding of a cold-worked Fe–2 at % Al alloy (data from [28]).

3.6. Transformation in Cu–Zn–Al shape-memory alloys [13]

Lee and Kim [13] studied the transformation in three Cu–Zn–Al shape-memory alloys by resistivity determinations for at least five temperatures per alloy. The alloys had been homogenized and quenched to obtain the β_1 (ordered) structure. In Table III the compositions of the three alloys are listed, together with the resulting microstructure after completion of the transformation, which was obtained from TEM. Lee and Kim [13] found that the transformation kinetics in alloys A and B could be well described by the AR equation, whilst those for alloy C fitted the JMAK equation well.

4. Discussion

In the previous section the transformation curves of several reactions which proceed by nucleation and growth were fitted with both the JMAK equation (Equation 1) and the AR equation (Equation 2). In all cases, better fits to the experimental data were obtained with the AR equation. In this section, the n values obtained from these fits are discussed.

4.1. Obtained *n* values for precipitation

TEM studies on Al–Li based alloys generally indicate that δ phase precipitates preferentially at grain boundaries but that it also precipitates in the grains [29–31]. Hence the overall evolution of the fraction transformed in the Al–2 mass % Li alloy is ascribed to a combination of grain-boundary precipitation and precipitation in the grain interior and Equation 14 should be employed. It has been shown before that for an Al–Li–Cu–Mg alloy, the lithium depletion of the grains close to the grain boundary is controlled solely by lithium diffusion to the grain boundary [32]. It is thought that this also holds for the binary Al–Li

TABLE III Summary of results obtained by Lee and Kim [13] for the transformation in three Cu–Zn–Al shape-memory alloys

Alloy	Cu	Zn	Al	Best fit *n*	Resulting structure (from TEM)
A	68.6	28.3	3.1	AR 2.5	Plates of α_1 bainite (9R structure)
B	71.8	23.1	5.1	AR 2.2	Plates of α_1 bainite (9R structure)
C	78.0	12.8	9.2	JMAK 2	Eutectoid-like structure with alternating lamellae of γ_2 (cubic) and α (FCC) phase

alloy and hence for this process $m_1 = n_1 = \frac{1}{2}$. For δ phase precipitation in the grain interior, it appears reasonable to assume a constant nucleation rate and hence $m_2 = 1\frac{1}{2}$, and $n_2 = 2\frac{1}{2}$. The data on the fraction transformed are fitted using Equations 12 and 14. The results presented in Fig. 2 show a close-to-perfect correspondence between theory and experiment. The two other curves in Fig. 2 are based on the assumption that only one of the two processes occurs and they show that grain-boundary precipitation is the most important process up to their cross-over point, whilst afterwards, nucleation in the grain interior becomes the dominating process of δ precipitation. This finding corresponds qualitatively with the following reasoning. The production process of Al–Li alloys used by Noble and Thompson [17] involved conventional casting, cold-rolling and solution-treatment at 580 °C. Hence, the alloys must possess a relatively large recrystallized grain size and this indicates that grain-boundary precipitation should be less important than nucleation and growth in the grain interior.

The same procedure with α_{ext} determined by two processes according to Equation 14, but with the relation between α and α_{ext} according to the JMAK method (i.e. Equation 11), also yields a good fit with the data, provided $n_2 = 1\frac{1}{2}$. However, this value indicates that δ phase precipitation in the grain interior would occur via site saturation. This appears unlikely, as δ phase is generally thought not to nucleate on precursors or on defects [30], i.e. there appears to be no reason why the number of nucleation sites of δ precipitates should be limited.

In summary, in the analysis for δ phase precipitation it is concluded that, in view of the fact that it is known that, for this reaction, both nucleation on the grain boundary and in the grains is important, Equation 14 in combination with either Equation 11 (from the JMAK theory) or Equation 12 with $c = 1$, gives the best results. As the fitting with the combination of Equation 12 with Equation 11 (impingement according to the JMAK model) yields an improbable value of n_2, it is thought that impingement with $c = 1$ (i.e. according to the AR model) is the correct description.

The reasoning applied above to δ phase precipitation has some general implications when the quality of fits are assessed. The application of Equation 14 as demonstrated in Fig. 2 shows that a deviation between fit and experimental data for low α may be due to an initial transformation process with a lower n value as compared to the dominating transformation process. In general, for all phases which can precipitate both in the grains and on the grain boundaries, this combination of processes can be expected to occur. Another example is a precipitation reaction where some product phase is already present at the start of the transformation. In such a case, precipitation on the already present product phase can initially be dominant, whilst later a second process may be dominant. This situation should arise in a liquid-quenched hypereutectic Al–Si alloy as in this alloy the matrix is supersaturated with about 2–3 at % Si whilst the remaining silicon is mainly present as finely dispersed silicon particles [33]. Hence, in Fig. 3 the deviations from the fit with AR equation at low α are interpreted as being due to initial precipitation on these finely dispersed silicon particles. This indicates that although the fit at low α is not good at all, still the experimental data in Fig. 3 are fully consistent with the treatment of impingement according to the AR equation. Also, it is clear that the precipitation of silicon from the aluminium-rich phase is a diffusion-controlled process, i.e. m should equal $1\frac{1}{2}$. It is further well known that nucleation of silicon precipitates occurs on sites where dislocation loops are present [34]. As these loops form before the transformation starts, all nucleation sites are thought to be used very early on in the transformation (i.e. a case of site saturation) and hence $n = m$. In accordance with this, the transformation data for the two Al–Si based alloys can be fitted either reasonably well (for Al–Si) or near perfectly (for Al–Si–Cu) to the AR equation and $n = 1\frac{1}{2}$. (Figs 3 and 4). As was argued above, the quality of the fit for the Al–Si alloy can be further improved by using Equation 14 in order to take account of some initial precipitation by growth of existing small silicon particles. This will remove the deviation between fit and data for small values of α. As the Al–Si–Cu alloy was produced via hot extrusion after solidification and subsequently solution-treated, this alloy will not contain a fine dispersion of silicon particles and no deviations of the fit of the AR equation at low α are expected. This is in agreement with the results obtained (see Fig. 4). Contrary to the good results obtained with the AR equations, the JMAK equation fits the data for the Al–Si based alloys very badly with $n = 1\frac{1}{2}$. A better fit (though still deficient for $\alpha > 0.75$) is obtained with $n = 1$, but following the reasoning put forward, $n < 1\frac{1}{2}$ is physically unreasonable.

Also for the formation of the Ll_2 phase in Al–15Mg cooled directly to the ageing temperature, the AR equation gave far better fits to experimental data compared to the JMAK equation. However, the n value obtained from the optimal fit with the AR equation (1.15, see Fig. 5) is somewhat lower than that expected for this diffusion-controlled reaction ($n = 1\frac{1}{2}$), which seems difficult to explain. It is suggested that coarsening in the latter stages of the reaction can be the reason for the somewhat low value of n. Within the concepts presented in Section 2, coarsening can be thought of as a process which reduces the number of growing nuclei, i.e. for the latter part of the transformation, $I(t)$ will be negative. Thus when coarsening occurs, the transformation rate will decrease as compared to the rate obtained with the AR equation, and n will decrease below $1\frac{1}{2}$. The obtained n values for the formation of Ll_2 ordered (δ′) phase in solution-treated and quenched Al–Li (Fig. 12 in [17]) and the Ll_2 ordered phase in melt-spun Al–Mg (Fig. 7b in [33]) (0.7 and 1, respectively) are not yet understood. However, as mentioned before, in both cases, the AR equation does provide better fits as compared to the JMAK equation.

In addition, for the internal nitriding of recrystallized Fe–2 at % Al, the AR equation yielded a better

fit as compared to the JMAK equation. The n value of 4 as obtained with the AR equation is slightly higher than the n value of 3.7 obtained by Biglari *et al.* [28], and the average n value of 3.5 obtained by Somers [35]. This small difference can be ascribed to the small difference between Equations 1 and 2 in the range $\alpha \in (0, 0.4)$ which was used by Biglari *et al.* and Somers for obtaining their n values (see Fig. 1). TEM experiments have shown [36] that AlN nucleates on dislocations and that new dislocations are generated during the precipitation, and hence one can expect the nucleation rate to increase with time. If the precipitation rate is determined by three-dimensional diffusion, whilst the nucleation rate increases approximately as t^a, then one would have $n = 1\frac{1}{2} + 1 + a$. Hence the measured n value of 4 indicates $a \approx 1\frac{1}{2}$. If this explanation is correct, one would expect that, for the cold-rolled alloy where a large amount of dislocations are present from the start of the precipitation process, the precipitation would correspond to three-dimensional diffusion-controlled precipitation for the site saturation case, i.e. $n = 1\frac{1}{2}$. This is indeed the n value found with the AR equation (see Fig. 7), and hence the present analysis of transformation curves of both cold-worked and recrystallized Fe–Al using the AR equation is fully consistent with the nucleation and diffusion-controlled growth mechanisms of AlN as put forward above. Further it is clear that the n value of 1 as obtained by Biglari and co-workers [28, 37], which is inconsistent with a reaction involving three-dimensional growth, is erroneous, because it was obtained using the JMAK equation in a range where it deviates strongly from the AR equation (α between 0.4 and 0.9).

Summarizing the analysis of nitriding of recrystallized and cold-worked Fe–2 at % Al with the aid of the AR equation (Equation 2) it is shown that:

(i) with the AR equation for both recrystallized and cold-worked Fe–2 at % Al, n values can be derived which are consistent with nucleation of AlN on dislocations and growth by three-dimensional diffusion; n values obtained with the JMAK equation are not consistent with a single nucleation and growth model; and

(ii) with the AR equation the data can be fitted over nearly the entire range of α; the JMAK equation can fit the data only up to $\alpha \approx 0.3$.

Hence with the AR equation, the analysis of the data is very much improved.

Using the AR equation, Lee and Kim obtained n values close to $2\frac{1}{2}$ for precipitation in their Cu–Zn–Al shape memory alloys A and B. These n values correspond to diffusion-controlled growth with constant nucleation rate.

In concluding this section, the results of the comparison of the applicability of the AR equation and the JMAK equation for the different precipitation reactions are gathered in Table IV. In all cases where one nucleation process occurs, the AR equation gave better fits than the JMAK equation. In the majority of cases, the n values are close to 1.5 or 2.5 and can be explained, by site saturated nucleation or nucleation at a constant rate.

TABLE IV Summary of precipitation reactions studied and the kinetic equation which fitted them best

Reaction[a]	Best fitting equation	Obtained n values
Precipitation of δ (AlLi) phase in WQ Al–Li	14	2.5
Precipitation in a LQ Al–Si alloy	AR/14	1.5
Precipitation in an WQ Al–Si–Cu alloy	AR	1.5
Formation of Ll_2 ordered phase in LQ Al–Mg	AR	1
Formation of Ll_2 ordered phase in WQ Al–Li	AR	0.7
Formation of Ll_2 ordered phase in AQ Al–Mg	AR	1.15
Internal nitriding of recrystallized Fe–2 at % Al	AR	4
Internal nitriding of cold-worked Fe–2 at % Al	AR	1.5
Transformation in Cu–28Zn–3 Al	AR	2.5
Transformation in Cu–23Zn–5 Al	AR	2.2

[a] LQ = quenched from liquid state by meltspinning; WQ = water quenched; AQ = cooled (quenched) in air.

4.2. Eutectoid reactions and autocatalytic reactions

The above analysis shows that for precipitation reactions the AR equation is more appropriate as the JMAK equation. It was noted by Lee and Kim [13] that the transformation in the Cu–13Zn–9Al alloy the JMAK equation (with $n = 2$) yields better fitting curves as compared to AR equation. Also, the fraction transformed during a perlitic transformation in a eutectoid steel can be fitted well with the JMAK equation and $n = 2.16$ [38]. In both cases, the resulting microstructure is lamellar eutectoid-like. According to the classic works on transformations in eutectoid steels (see [39]), a perlitic structure, which, in steels, is a combination of alternating plates of Fe_3C and α-iron, nucleates from the austenite by the formation of one of the two phases (Fe_3C in steels) on grain boundaries. Next the Fe_3C grows and α-iron nucleates on it, and this combination of one lamella of Fe_3C and one lamella of α-iron can be considered to be the first fully transformed region. Subsequent formation of transformed regions occurs mainly by nucleation on previously transformed regions in such a way that the characteristic alternating lamellar structure is obtained. Hence this transformation process is autocatalytic: nucleation occurs on previously transformed regions. The assumption of random nucleation made in the derivation of the JMAK equation is clearly not valid here, and the good fit between the JMAK equation and the experimental data for the autocatalytic eutectoid reactions may be fortuitous. This point is discussed in the following paragraph.

In an autocatalytic eutectoid-like reaction, new reaction products nucleate on the surfaces of pre-existing products, and hence it can be assumed that the growth of each product will effectively be halted when most of its surface is covered by newly nucleated product. If the nucleation rate per unit of surface, I_s is assumed constant, this means that each product

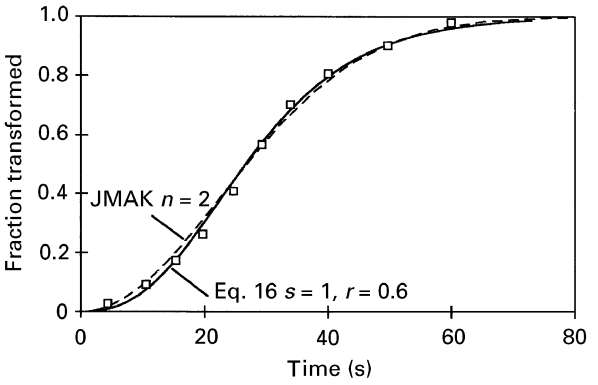

Figure 8 Fraction transformed during the perlitic transformation in a eutectoid steel. The ability of the JMAK equation and Equation 16 (with $s = 1$) to fit the data is nearly equal (data from [38]).

will grow for an approximately fixed time interval, τ, to attain an approximately constant volume. Hence, the reaction rate can be approximated as

$$\frac{d\alpha}{dt} = B_1 I_s S(t - \tau_d) \quad (15)$$

where $S(t)$ is the surface area of the reaction product available for nucleation, $\tau_d < \tau$, B_1 is a constant. Before impingement becomes important, S will be proportional to α^r, with $r \approx \frac{2}{3}$. Later on, the surface area available will be reduced by impingement. To correct for this, it is simply assumed that S is proportional to $\alpha^r(1 - \alpha)^s$, where s is expected to be close to unity. Hence it follows that

$$\frac{d\alpha}{dt} = B_2 I_s[\alpha(t - \tau_d)]^r[1 - \alpha(t - \tau_d)]^s \quad (16)$$

where B_2 is a constant. It can be shown that transformation curves obtained with the latter equation are very similar to transformation curves obtained with the JMAK equation. For instance, with $\tau_p = 0$, $r = 1 - 1/n$ and $s = 0.774$, 0.7, 0.664 for $n = 2$, 3, 4, transformation curves which are practically indistinguishable from JMAK curves can be obtained (see also [40]). Also, with $s = 1$, curves which are quite similar to JMAK curves over a large range of α values can be obtained. In order to give a specific example of how Equation 16 can explain observed transformation curves, the data on the perlitic transformation in eutectoid steel (from [38]) has been fitted with Equation 16 taking $s = 1$ and $\tau_p = 0$. The result, presented in Fig. 8, shows that with $r = 0.6$, Equation 16 gives a fit $\alpha > 0.15$ which is even somewhat better than the JMAK fit. The marginally worse quality of the fit for $\alpha < 0.15$ is not surprising if one considers that for this stage of the reaction little surface area is available for the autocatalytic process, and hence nucleation is probably dominated by another mode of nucleation. (In the eutectoid steel this process would be grain-boundary nucleation.)

5. Conclusion

It has never been proved that the JMAK equation can fit data of diffusion-controlled precipitation reactions. In this work, the ability of the JMAK equation to fit such experimental data has been compared with the Austin–Rickett (AR) equation

$$\alpha = 1 - \{[k(T)t]^n + 1\}^{-1} \quad (2)$$

In most cases, the AR equation immediately provided a better fit to the data (see Table IV) and the obtained integer and half-integer values of n could be interpreted consistently in terms of the physics of the transformation processes. The latter is mostly not possible for n values obtained from the JMAK equation. It is concluded that the AR equation is more appropriate in interpreting data of precipitation reactions than the JMAK equation.

Acknowledgements

This work is financed in part by the EC Human Capital and Mobility project. Dr A.-M. Zahra is thanked for stimulating discussions.

References

1. W.A. JOHNSON and K.E. MEHL, *Trans. Am. Inst. Min. Met. Eng.* **195** (1939) 416.
2. M. AVRAMI, *J. Chem. Phys.* **9** (1941) 177.
3. *Idem, ibid.* **7** (1939) 1103.
4. *Idem, ibid.* **8** (1940) 212.
5. A.N. KOLMOGOROV, *Izv. Akad. Nauk SSSR, Ser. Mater.* **1** (1937) 355.
6. J.W. CHRISTIAN, "The Theory of Transformation in Metals and Alloys", 2nd Edn., Part 1 (Pergamon Press, Oxford, UK, 1975).
7. GE YU and J.K.L. LAI, *J. Appl. Phys.* **79** (1996) 3504.
8 R.A. VANDERMEER and P. GORDON, in "Recovery and Recrystallization in Metals", edited by L. Himmel (Gordon and Breach Science, New York, NY, 1963) p. 211.
9. S. BRAUER, J.O. STRÖM-OLSEN, M. SUTTON, Y.S. YANG, A. ZALUSKA, G.B. STEPHENSON and U. KÖSTER, *Phys. Rev. B* **45** (1992) 7704.
10. N.X. SUN, X.D. LIU and K. LU, *Scripta Mater.* **34** (1996) 1201.
11. F.S. HAM, *Q. J. Appl. Math.* **17** (1959) 137.
12. *Idem, J. Appl. Phys.* **30** (1959) 1518.
13. EON-SIK LEE and YOUNG G. KIM, *Acta Metall. Mater.* **38** (1990) 1669.
14. J.B. AUSTIN and R.L. RICKETT, *Trans. Am. Inst. Min. Eng.* **135** (1939) 396.
15. V. ERUKHIMOVITCH and J. BARAM, *Phys. Rev. B* **50** (1994) 5854.
16. *Idem, ibid.* **51** (1995) 6221.
17. B. NOBLE and G.E. THOMPSON, *Metal Sci. J.* **5** (1971) 114.
18. P. VAN MOURIK, E.J. MITTEMEIJER and TH. H. DE KEIJSER, *J. Mater. Sci.* **18** (1983) 2706.
19. P. VAN MOURIK, PhD Thesis, Delft University of Technology (Delft University Press, Delft, The Netherlands, 1988).
20. J.L. MURRAY and A.J. McALISTER, *Bull. Alloy Phase Diagr.* **5** (1984) 74.
21. M.J. STARINK, P. VAN MOURIK and B.M. KOREVAAR, *Metall. Trans.* **24A** (1993) 1723.
22. J.L. MURRAY, *Int. Metall. Rev.* **30** (1985) 211.
23. M.J. STARINK and P. VAN MOURIK, *Mater. Sci. Eng.* **A156** (1992) 183.
24. *Idem, J. Mater. Sci.* **29** (1994) 2835.
25. A.-M. ZAHRA and M.J. STARINK, unpublished research (1996).
26. M.J. STARINK and A.-M. ZAHRA *Mater. Sci. Forum* **217–222** (1996) 795.
27. M. VAN ROOYEN, J.A. SINTE MAARTENSDIJK and E.J. MITTEMEIJER, *Metall. Trans.* **19A** (1988) 2433.

28. M.H. BIGLARI, C.M. BRAKMAN, E.J. MITTEMEIJER and S. VAN DER ZWAAG, *Metall. Mater. Trans.* **26A** (1995) 765.
29. K. SATYA PRASAD, A.K. MUKHOPADHYAY, A. A. GOKHALE, D. BANERJEE and D.B. GOEL, *Scripta Metall. Mater.* **30** (1994) 1299.
30. O. JENSRUD and N. RYUM, *Mater. Sci. Eng.* **64** (1984) 229.
31. P.J. GREGSON and S.A. COURT, *Scripta Metall. Mater.* **30** (1994) 1359.
32. M.J. STARINK and P.J. GREGSON, *Mater. Sci. Eng.*, **A211** (1996) 54.
33. M. VAN ROOYEN and E.J. MITTEMEIJER, *Metall. Trans.* **20A** (1989) 1207.
34. E. OZAWA and H. KIMURA, *Mater. Sci Eng.* **8** (1971) 327.
35. M.A.J. SOMERS, PhD thesis, Delft University of Technology, Delft, The Netherlands (1989) Ch.II.
36. H.H. PODGURSKI and H.W. KNECHTEL, *Trans. AIME* **245** (1969) 1595.
37. J.S. STEENAERT, M.H. BIGLARI, C.M. BRAKMAN, E.J. MITTEMEIJER and S. VAN DER ZWAAG, *Z. Metallkde* **86** (1995) 700.
38. E. GAUTIER, A. SIMON and G. BECK, *Acta Metall.* **35** (1987) 1367.
39. H. SCHUMANN, "Metallographie" (Fachbuchverlag Leipzig, Leipzig, Deutschland, 1958).
40. TONG B. TANG and M.M. CHAUDHRI *J. Thermal. Anal.* **17** (1979) 359.
41. G. POKOL and G. VÁRHEGYI, *CRC Crit. Rev. Anal. Chem.* **19** (1988) 65.

Received 14 June 1996
and accepted 28 January 1997